CHEMISTRY
A EUROPEAN JOURNAL

DOI: 10.1002/chem.200802373

Linker Conjugation Effects in Rhenium(I) Bifunctional Hole-Transport/Emitter Molecules

Deidre M. Cleland,[a] Garth Irwin,[a] Pawel Wagner,[b] David L. Officer,[b] and Keith C. Gordon*[a]

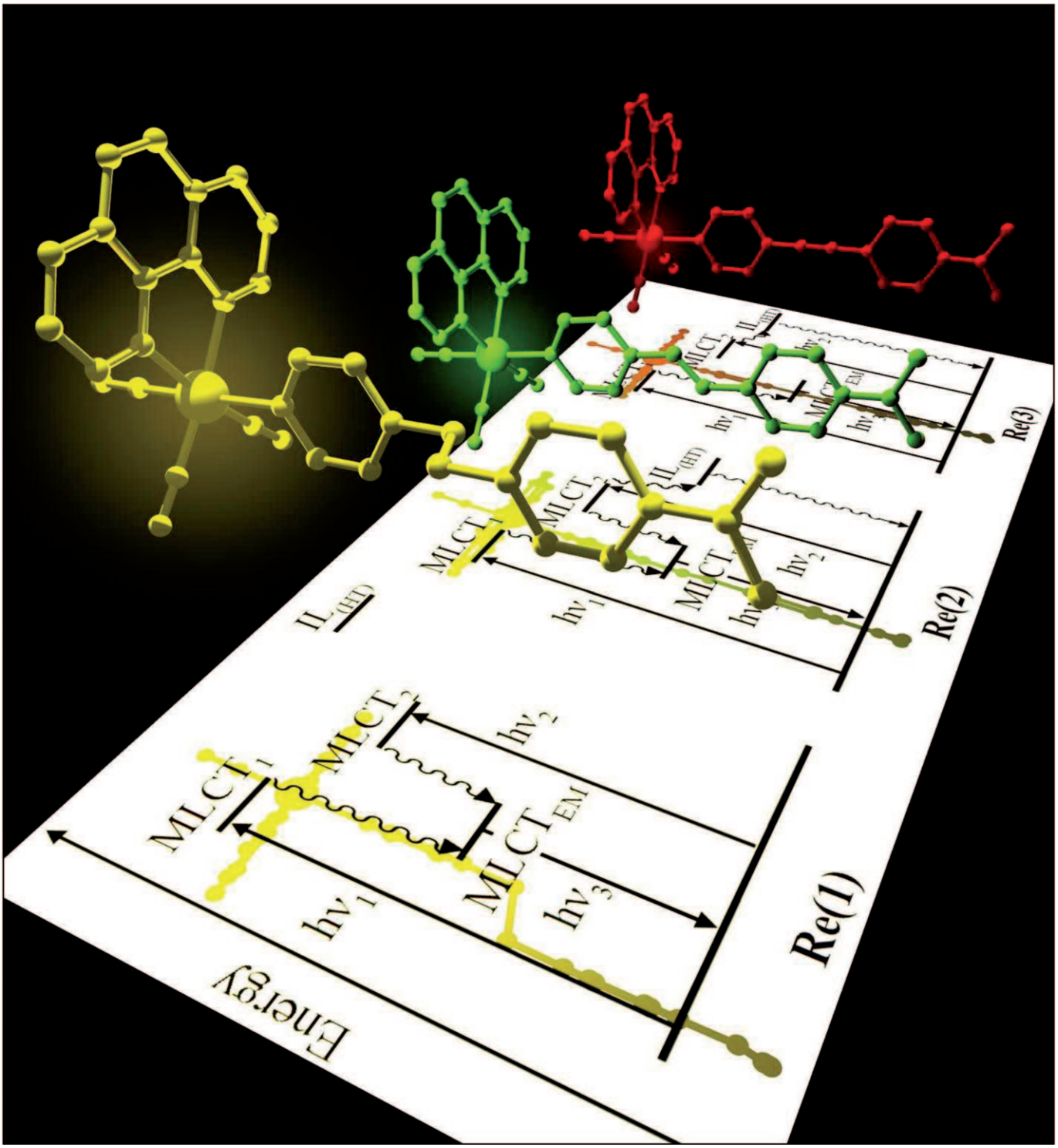

Abstract: Spectroscopic, electrochemical and density functional theory (DFT) methods have been employed to investigate a group of $[Re(CO)_3(HT)(phen)]^+$ complexes (phen = 1,10-phenanthroline), and in particular the level of electronic communication between various hole-transporting (HT) ligands and the rhenium centre. Here, the HT ligand consists of a coordinating pyridine connected to dimethylaniline group through a single-, double- or triple-bond-connecting system. Electronic absorption, resonance Raman, and steady-state emission spectroscopy combined with lifetime studies and DFT calculations suggest that multiple $d\pi(Re)\rightarrow\pi^*(phen)$ metal-to-ligand charge transfers (MLCTs) exist for each complex, two of which significantly absorb at about 340 and 385 nm, and one that emits at approximately 540 nm. In the complexes containing more-conjugated HT ligands, non-emissive intraligand transitions ($IL_{(HT)}$) exist with energies between the ground and MLCT excited states. The overlap of these $IL_{(HT)}$ transitions and the absorbing MLCT of lowest energy deactivates emission resulting from about 385 nm excitation, and lowers the quantum yield and excited-state lifetimes of these complexes. Cyclic voltammetry experiments indicate that throughout the series investigated, the highest occupied molecular orbital (HOMO) of each complex is centred on the HT ligand, while the occupied molecular orbitals localised on the rhenium are lower in energy.

Keywords: electrochemistry · electronic structure · light-emitting diodes · UV/Vis spectroscopy · transition metals

Introduction

Since the first organic light emitting diode (OLED) was shown to exhibit high emission efficiency, fast response and a low turn on voltage,[1] considerable research has focused on developing OLED materials that further optimise these parameters. The majority of those investigated have been based on the multilayer device structure employed by Tang and VanSlyke (similar to Figure 1).[1,2] However, while some of these exhibit promising characteristics, the best often involve layered structures more complex than that of Figure 1, and there is still room for improvement in regards to the key operation parameters.[3,4]

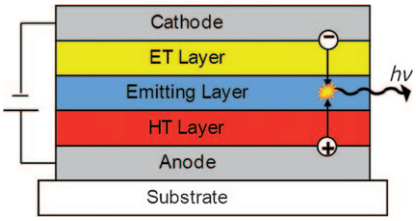

Figure 1. The basic structure of a typical multilayer OLED device. Electrons and holes move through the electron-transporting (ET) and hole-transporting (HT) layers, respectively, to recombine on the emitting layer, form an exciton and radiatively decay.

This study looks at an alternate approach to the design of OLED materials in which the hole-transporting (HT), electron-transporting (ET) and emissive layers shown in Figure 1 are reduced to functional groups within a trifunctional molecule (Figure 2a). The hypothesis is that the trifunctional molecules act in a similar fashion to a multilayer device. When a potential is applied, electrons are injected into the lowest unoccupied molecular orbital (LUMO) of the ET moiety and holes into the highest occupied molecular orbital (HOMO) of the HT moiety. These charges then travel towards the emissive functional group where they recombine, form an exciton, and decay to produce the observed light emission (Figure 2b).[5]

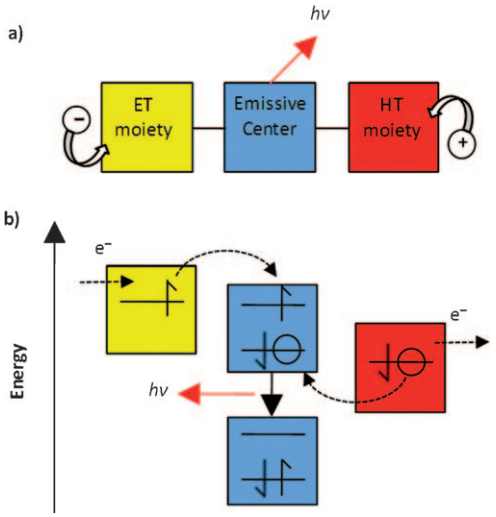

Figure 2. The function of each moiety within a trifunctional OLED molecule.

Use of these trifunctional compounds will reduce the number of layers required in OLEDs, resulting in simpler

[a] D. M. Cleland, Dr. G. Irwin, Prof. K. C. Gordon
Department of Chemistry and
MacDiarmid Institute for Advanced Materials and Nanotechnology
University of Otago, Union Place
PO Box 56, Dunedin (New Zealand)
Fax: (+64) 3-479-7906
E-mail: kgordon@chemistry.otago.ac.nz

[b] Dr. P. Wagner, Prof. D. L. Officer
ARC Centre of Excellence for Electromaterials Science
Intelligent Polymer Research Institute
University of Wollongong
Wollongong NSW 2522 (Australia)

device fabrication. Also, in principle these compounds may improve the efficiency and balance of charge injection into an OLED device, while promoting recombination at the appropriate emissive site.[6–9] In order to be effective, trifunctional molecules must be designed so that the orbital energies of each functional group encourage the required charge transfer, while maintaining an appropriate level of electronic communication across the molecule. At present, the molecular characteristics that result in these properties are poorly understood.[7] This study looks at a group of hole-transporting/emissive centre molecules shown in Figure 3 (**1**–**3**), in an attempt to provide some insight into the nature of the HT ligand/emissive centre interaction. This study is not directly concerned with producing the optimal OLED materials.

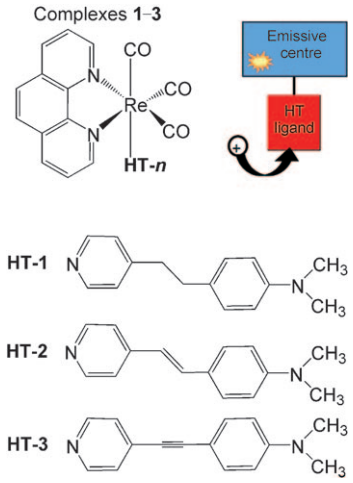

Figure 3. The combination of emissive centre and HT ligand for the molecules investigated in this project.

A rhenium(phenanthroline) {Re(phen)} group was chosen as the emissive centre becuase of its high quantum yield.[10,11] The associated carbonyls are also useful spectroscopic tools in studies of this nature.[12] The tertiary amine group provides a site for hole injection,[13,14] and this is connected to a coordinating pyridine through a bonding network of variable conjugation. It is expected that the level of conjugation between the HT group and metal centre will have some effect on the charge communication across the two functionalities, although the extent and consequences of this effect are unknown and thus the focus of this investigation.

Spectroscopic and electrochemical techniques were employed to examine the vibrational, electronic and redox properties of the bifunctional complexes. DFT calculations were also performed to aid in the interpretation of physical results. To help identify a HT-ligand/emissive-centre interaction when present, each of the bifunctional compounds were additionally compared to isolated HT and emissive systems. These were represented by the uncoordinated HT ligands of the respective complexes and $[Re(CO)_3(4\text{-methylpyridine})(phen)]^+$ (**4**), which is essentially an unperturbed emissive centre.

Results and Discussion

To establish that the DFT computational method is accurate in modelling the molecules investigated here, the IR and FT-Raman spectra were calculated from an optimised molecular geometry, and compared to experimentally obtained data. The level of correlation was then quantified by using the mean absolute deviation (MAD) between the frequencies of the most intense peaks.[15] Calculated frequencies were scaled by 0.970, as this value produced the lowest MADs; this scale factor has been found to be optimal for scaling polypyridyl vibrations.[16] An example of a calculated/experimental FT-Raman comparison is shown for **2** in Figure 4. This data is considered to show good correlation with regards to the position and intensity of peaks, and has a MAD of 8 cm^{-1}.

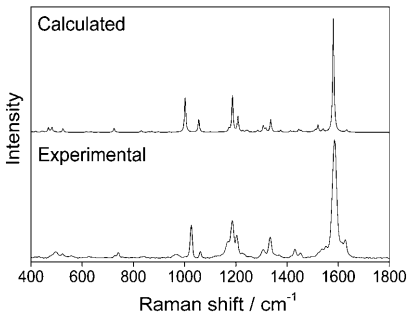

Figure 4. Comparison between the experimental and calculated FT-Raman spectra of **2**. The calculated spectrum was obtained using the B3LYP/6-31G(d) DFT computational method (with the LANLDZ basis set on the Re atom) and frequencies were scaled by 0.970. The experimental spectrum was recorded from solid-state **2** with $\lambda_{ex} = 1064$ nm.

One anomaly in these results was in the poorer agreement of theoretical spectra with experimental data for the singly bonded systems. This situation was not improved by altering the starting geometries. The disparity was attributed to the tendency of the B3LYP level of theory to overestimate the importance of conjugation.[17] However, experimental data from complex **1** is very similar to that of **4**. This suggests that with the singly bonded connecting system, the tertiary amine substituent of **1** has a minimal effect on the molecule. Empirical comparisons to calculations on complex **4** can therefore be made to compensate for any inaccuracies in the DFT results of **1**.

The low-energy UV/Vis transitions observed for the free ligands and complexes are given in Table 1. In addition to these, an intense absorption ($\varepsilon \approx 4 \times 10^4$ $L\,mol^{-1}\,cm^{-1}$) is evident in the spectra of all Re complexes at around 277 nm. From comparison to literature, this was assigned to an intraligand $\pi \rightarrow \pi^*$ phenanthroline ($IL_{(phen)}$) transition.[18] The wavelength invariance of this transition with the various HT

ligands suggests that any effect the change in conjugation on the Re moiety does not appear to extend to the phen ligand.

The low-energy shoulder at 338 nm in the spectrum of **4** has been previously assigned to a $d\pi(Re)\rightarrow\pi^*$(phen) metal-to-ligand charge transfer (MLCT).[18] The similarity of this to the shoulder in the spectrum of complex **1**, with regards to wavelength and extinction coefficients, suggests that **1** possesses a similar $d\pi(Re)\rightarrow\pi^*$

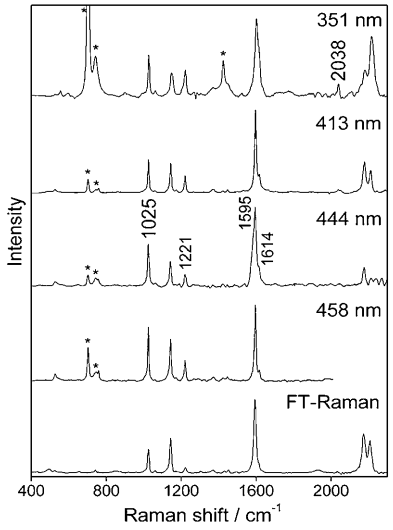

Figure 6. The resonance Raman spectra of **3** (ca. 10^{-3} M in CH_2Cl_2) obtained using excitation wavelengths that probe the low-energy, electronic absorption band (351, 413, 444 and 458 nm). These are compared to the solid-state FT-Raman spectrum ($\lambda_{exc}=1064$ nm). * indicates solvent bands.

MLCT transitions that may be present. However, the carbonyl peak does suggest a minor contribution from an MLCT-like transition at higher energies.

The excited state parameters for the complexes are shown in Table 2. The single **4** emission band at 540 nm has been

Table 2. Excited state lifetimes, quantum yields and associated parameters.[a]

	Em. λ_{max} [nm]	Excit. λ [nm]	Lifetime τ [μs]	Quantum yield ϕ	k_r[b] [10^4 s^{-1}]	k_{nr}[c] [10^4 s^{-1}]
4	540	343, 388	0.98	0.262	26.7	75.1
1	538	340, 386	1.30	0.135	10.4	66.3
2	528	341, 384	1.23	0.079	6.42	74.6
3	531	345, 385(sh)	1.04	0.055	5.27	90.6

[a] Solutions were ca. 10^{-5}–10^{-6} M (CH_2Cl_2). Lifetime values are the mean of three measurements using 355 nm excitation, correlated to [Ru(bipy)$_3$]$^{2+}$ (0.58 μs at 25°C).[29] Quantum yields were calculated following the methods of Wang et al.[30] but with quinine sulfate as the standard ($\phi=0.546$).[31] [b] k_r = radiative rate constant [s^{-1}]. [c] k_{nr} = non-radiative rate constant [s^{-1}].

similarly observed by Sacksteder et al.,[18] who assigned it to a dπ(Re)←π*(phen) emission from a MLCT excited state. As can be seen in Figure 7, the excitation spectrum is likewise coincident with the UV/Vis shoulder previously assigned to MLCT absorption; however, the excitation spectrum is clearly split into two peaks that lie at approximately 340 and 385 nm. It is thus assumed that multiple MLCT excited states exist for **4**, two of which are close in energy and significantly absorbing ($MLCT_1$ and $MLCT_2$ in Figure 8) and one that is emissive ($MLCT_{EM}$). Molecules excited into either of the two absorbing MLCT states decay non-radiatively to emit from the third. Time-dependent DFT calculations support this prediction, indicating the presence of multiple MLCT transitions. Two of these have substantial oscil-

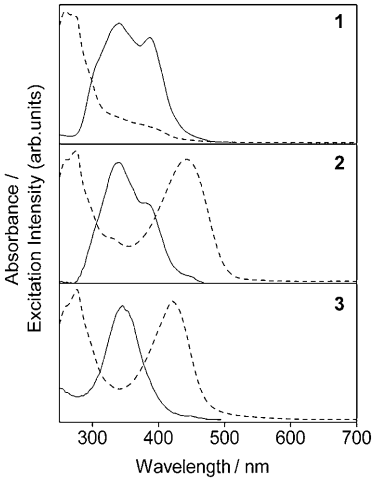

Figure 7. The excitation (——) and electronic absorption (-----) spectra of the rhenium complexes. Solutions were typically 10^{-5} M (CH_2Cl_2), but spectra were scaled for comparison.

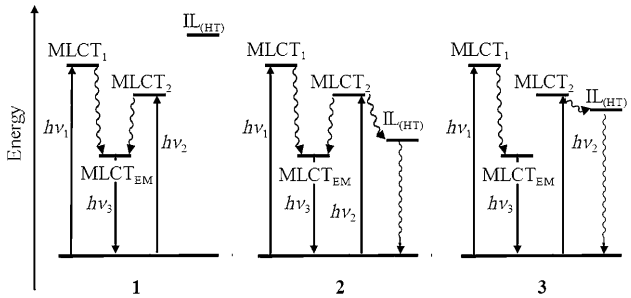

Figure 8. Simplified energy diagram for **1**, **2** and **3**, representing the radiative (straight arrows) and non-radiative (wavy arrows) decay pathways from the MLCT excited states.

lator strengths and likely correspond to the two absorbing states, while lower energy forbidden transitions are also predicted, any of which could be responsible for the emissive state.

The broad, unstructured nature of the **4** emission is typical of a rhenium MLCT excited state,[19] and these characteristics are evident in the spectra of all complexes. Furthermore, the excitation energies recorded in Table 2 are similar to that of **4** and essentially constant throughout the molecule series. These are aligned with the shoulder in the UV/Vis spectrum of **2**, but do not correspond to the intense $IL_{(HT)}$ bands in either **2** or **3**. These results are finally solid evidence for the presence of low-energy MLCT transitions within the UV/Vis spectra of these complexes, and all emissions are thus attributed to radiative decay from an MLCT excited state. The results also suggest that despite often being the lowest in energy, the $IL_{(HT)}$ excited states are non-emissive.

While the excitation peak positions remain constant, the intensity of the low-energy band significantly decreases across the molecule series (Figure 7). A significant drop in the quantum yields of **2** and **3** is also observed. It is possible these results are due to inner filter effects produced by the

highly absorbing $IL_{(HT)}$ transitions; however, this seems unlikely as the measurements were taken from very dilute solutions. For example, the decreased peak intensity and quantum yield are most severe for **3**; however, the solution from which this was measured had a concentration of only 2.5×10^{-6} mol L^{-1}. This means that even after travelling the full length of the cell over 90% of the incident excitation light remains,[27,28] and the small decrease that does occur can certainly not account for the effects recorded in Table 2.

These can instead be attributed to the low energies of the $IL_{(HT)}$ states in the more conjugated HT ligands.[29,30] The non-emissive states provide alternative, non-radiative pathways for decay from $MLCT_2$ as is depicted in Figure 8. The consequence is to essentially "switch off" the emission resulting from lower energy MLCT excitation, and the complexes are forced to emit solely via the $MLCT_1$ excited state. The associated decrease in quantum yields is clearly unfavourable if molecules of this nature are to be considered for use in OLEDs. The large rate of non-radiative decay for **2** and **3** also decreases the excited state lifetimes of these complexes relative to that of **1**.[27] However as expected, the relatively long lifetimes of all complexes shown in Table 2 are similar to that of typical $d\pi(Re)\rightarrow\pi^*(phen)$ MLCT excited states.[31]

Of the two complexes containing conjugated HT ligands, the decrease in quantum yield, lifetime, and subsequent effects are more exaggerated for **3**. This can be attributed to the slightly higher energy of the **3** $IL_{(HT)}$ transition relative to that of **2** (Figure 8). The $MLCT_2$ and $IL_{(HT)}$ states of **3** are therefore closer in energy, resulting in larger overlap, and more effective deactivation of $MLCT_2$ (Figure 8). These results are in accordance with the energy-gap law with regards to the $IL_{(HT)}$ and $MLCT_2$ excited states, as is to be expected for Re MLCT compounds.[32,33]

Finally, the drop in quantum yield of **1** relative to **4** does suggest that despite being higher in energy, the $IL_{(HT)}$ transition of **1** is close enough to the MLCT states for some degree of overlap to exist. Although this interaction is much less significant than that of **2** and **3**.

While the oxidation potential of the free HT ligand of complex **2** could not be established due to surface phenomena, the first oxidation peaks of complexes **1** and **3** appear at similar potentials to that of their respective free ligands (Table 3). The first oxidations of the rhenium complexes are consequently attributed to removal of an electron from their HT ligands. From comparison to literature values for the oxidation of various tertiary amines, the peaks are more specifically attributed to localised oxidation of the tertiary amine moiety of the HT ligands.[36,37] This assignment implies that the tertiary amine moieties are serving their purpose of providing a site for hole injection into the molecule.

Table 3. The peak potentials (vs. SCE) of the ligands and complexes investigated here (10^{-3} M CH_2Cl_2 with 0.1 M TBAP). Cyclic voltammograms were recorded at 1 Vs^{-1} and calibrated against the DMFc couple. Solutions were typically 1 mM. All peak potentials were irreversible. The oxidation of **HT-2** is concealed by surface phenomena and is not reported

	E^1_{ox} [V]	E^2_{ox} [V]
HT-1	0.97	–
HT-2	–	–
HT-3	1.18	–
4	–	1.85
1	1.03	1.92
2	0.93	1.94
3	1.13	1.96

Only one oxidation peak appears in the cyclic voltammogram of **4** at a potential of 1.85 V. This is in a very similar position to that recorded for the same compound by Sacksteder et al. (1.81 V vs. SCE), who assigned the peak to oxidation of the rhenium atom from Re^{I} to Re^{II}.[18] The irreversibility and high potential of this oxidation is typical of rhenium polypyridyl complexes,[38] thus the second oxidation peaks in Table 3 are all assigned to the $Re^{II/I}$ couple.

The relative potentials of the two oxidation peaks of each complex suggest the tertiary amine occupied orbitals lie at higher energies than the highest occupied metal-based orbital. For example, by using the methods of Li et al.,[39] the HT moiety and Re-centred HOMOs for **3** are calculated to lie at −5.3 and −6.0 eV, respectively.

The small oxidation potentials of the HT ligands have some advantages in that they introduce the possibility of a low OLED turn-on voltage. Furthermore, the separate nature of the two oxidations implies in the ground state the HT and metal moieties are electronically isolated. To some extent this is desirable for multifunctional OLED compounds as localised holes need to be injected into the HT functionality and then move to the emissive centre, rather than the positive charge delocalising across the entire molecule.

However because holes move through HOMOs of increasing energy the relative orbital energies of these bifunctional complexes are not conducive to OLED applications.[2] Instead of promoting hole transportation to the metal centre for exciton formation, the relative orbital ordering causes the triphenyl amine group to act as a hole trap, a property that is of little use in OLED applications.

Conclusions

Once it was established that the B3LYP DFT method was providing an accurate model for most molecules studied in this project, calculated properties could aid in the interpretation of physical measurements. These indicated the presence of multiple low-energy excited states in each bifunctional complex, including a dark $IL_{(HT)}$ transition and various $d\pi(Re)\rightarrow\pi^*(phen)$ MLCT excited states, two of which absorb significantly to emit from a third. The major source of HT ligand/emissive centre interaction was found to be the proposed overlap of the $IL_{(HT)}$ excited state with the absorbing MLCT transition of lower energy. This effect was consistent with the observed excited state properties, and was most significant in the complexes containing conjugated HT ligands in which the $IL_{(HT)}$ transition energy was sufficiently lowered for substantial overlap to occur. One conse-

quence of the non-radiative pathway provided by the $IL_{(HT)}$ transitions is the drop in quantum yield for complexes **2** and **3**, an effect that is undesirable when considering these compounds in the context of OLED applications. This may be rectified by using a different metal centre that is easier to oxidise, such as ruthenium(II).

Finally, cyclic voltammetry investigations revealed that the rhenium based HOMO lies at lower energies than that localised on the HT ligands. The relative energies of the two moieties are thus opposed to that required for hole transfer to the metal centre, and this result is likewise unfavourable in regards to OLED applications.

Experimental Section

***N,N*-Dimethyl-4-(2-pyridin-4-ylvinyl)aniline (HT-1)** was synthesised according to literature.[40–42] The other starting materials were commercially available and used without further purification except potassium *tert*-butoxide, which was purified by sublimation. Some of carbon NMR signals overlapped and the spectra appear as described.

***N,N*-Dimethyl-4-(2-pyridin-4-ylethyl)aniline (HT-2)**: *N,N*-Dimethyl-4-(2-pyridin-4-ylvinyl)aniline (0.224 g, 1 mmol) was dissolved in formic acid (20 cm^3), 10% Pd/C was added (0.224 g) and the resulting mixture was stirred at 60 °C for 2 h under a hydrogen atmosphere. Afterwards the catalyst was filtered off and the resulting clear solution was neutralised by conc. ammonia. The resulting white fine needles were filtered off, washed by water and dried (0.198 g, 88%). The spectroscopic data were compared to reported in literature.[43]

***N,N*-Dimethyl-4-(pyridin-4-ylethynyl)aniline (HT-3)**: The preocedure was modifed from the literature synthesis.[41] Diphenyl-1-chloro-1-(4-pirydyl)-methanephosphonate (0.724 g, 2 mmol) and 4-(*N,N*-dimethylamino)benzaldehyde (0.328 g, 2.2 mmol) were dissolved in dry THF (40 cm^3), then potassium *tert*-butoxide (0.505 g, 4.5 mmol) was added in one portion. The resulting yellow mixture was stirred at RT for 3 h and then poured into of ice-cold water (150 cm^3). The yellow fine needles were filtered off and dried. The yellow solid was dissolved in 10% solution of KOH in MeOH (50 cm^3) and heated under reflux for an additional 2 h. Afterwards the mixture was poured into water (200 cm^3) and the yellow solid was filtered off then dried. After purification on silica with diethyl ether as an eluent, a yellow powder was obtained which was recrystallised from diethyl ether/hexane mixture to give the product (0.141 g, 31%).[44]

Synthesis of the *fac*-[Re(CO)$_3$(HT)(phen)] complexes: These complexes were prepared based on established literature procedures.[6,16,18,33,45] Commercially obtained $[Re(CO)_5Cl]$ (Aldrich) and 1,10-phenanthroline·H_2O (Aldrich) were heated under refluxed in absolute ethanol to give *fac*-$[Re(CO)_3Cl(phen)]$. This was subsequently converted to *fac*-$[Re(CO)_3(MeCN)(phen)]PF_6$ by refluxing with $AgPF_6$ in MeCN, filtering off the solid AgCl and evaporating the solvent under reduced pressure. The *fac*-$[Re(CO)_3(HT)(phen)]PF_6$ complexes were prepared from *fac*-$[Re(CO)_3(MeCN)(phen)]PF_6$ by heating under reflux in THF under nitrogen with a molar equivalent of the appropriate ligand; the preparation of *fac*-$[Re(CO)_3(4\text{-}Mepy)(phen)]$ is given as a representative example.

fac-*[Re(CO)$_3$(4-methylpyridine)(phen)]PF$_6$* (***4***): *fac*-$[Re(CO)_3(MeCN)(phen)]PF_6$ (100 mg, 0.16 mmol) and 4-methylpyridine (15 mg, 0.16 mmol) were heated under reflux in THF (10 mL) under nitrogen for 8 h. The solution was then cooled and the solvent removed by evaporation under reduced pressure to give a yellow solid. The solid was then suspended in water (10 mL) before being filtered, washed with water (10 mL portions), isopropanol and diethyl ether and then air dried. Yellow solid; yield 99 mg (94%); ^{1}H NMR (300 MHz, [D$_6$]acetone, 25 °C): $\delta = 2.23$ (s, 3H), 7.17 (d, $^3J(H,H) = 6.6$ Hz, 2H), 8.30–8.36 (m, 2H), 8.37 (s, 2H), 8.42 (d, $^3J(H,H) = 6.6$ Hz, 2H), 9.10 (d, $^3J(H,H) = 8.4$ Hz, 2H), 9.90 ppm (d, $^3J(H,H) = 8.4$ Hz, 2H); MS (ESI POS): *m/z* (%): 544.0699 $[M]^+$, 451.0139 $[Re(CO)_3(phen)]^+$; elemental analysis calcd (%) for $C_{21}H_{15}N_3O_3RePF_6$: C 36.63, H 2.20, N 6.10; found: C 36.71, H 2.28, N 6.12.

fac-*[Re(CO)$_3$(**HT-1**)(phen)]PF$_6$* (***1***): Orange-brown solid; yield 85%; ^{1}H NMR (300 MHz, [D$_6$]acetone, 25 °C): $\delta = 2.65$ (t, $^3J(H,H) = 8.1$ Hz, 2H), 2.79 (t, $^3J(H,H) = 8.1$ Hz, 2H), 6.75 (d, $^3J(H,H) = 8.7$ Hz, 2H), 6.85 (d, $^3J(H,H) = 8.7$ Hz, 2H;), 7.15 (d, $^3J(H,H) = 6.3$ Hz, 2H), 8.35 (m, 6H), 9.10 (d, $^3J(H,H) = 8.4$ Hz, 2H), 9.89 ppm (d, $^3J(H,H) = 5.1$ Hz, 2H), *N*-methyl peak was not assigned as it appeared to overlap with the residual water peak at 2.85 ppm; MS (ESI POS): *m/z* (%): 677.1578 $[M]^+$, 451.0119 $[Re(CO)_3(phen)]^+$; elemental analysis calcd (%) for $C_{30}H_{26}N_4O_3RePF_6$: C 43.85, H 3.19, N 6.82; found: C 43.69, H 3.36, N 6.43.

fac-*[Re(CO)$_3$(**HT-2**)(phen)]PF$_6$* (***2***): Orange solid; yield 87%; ^{1}H NMR (300 MHz, [D$_6$]acetone, 25 °C): $\delta = 2.98$ (s, 6H), 6.72–6.77 (m, 3H), 7.31–7.39 (m, 5H), 8.34–8.36 (m, 6H), 9.10 (d, $^3J(H,H) = 8.4$ Hz, 2H), 9.89 ppm (d, $^3J(H,H) = 5.1$ Hz, 2H); MS (ESI POS): *m/z* (%); 675.1387 $[M]^+$, 451.0083 $[Re(CO)_3(phen)]^+$; elemental analysis calcd (%) for $C_{30}H_{24}N_4O_3RePF_6 \cdot H_2O$: C 43.01, H 3.13, N 6.69; found: C 43.08, H 2.99, N 6.59.

*fac-[Re(CO)$_3$(HT-**3**)(phen)]PF$_6$* (***3***): Brown solid; yield 93%; ^{1}H NMR (300 MHz, [D$_6$]acetone, 25 °C): $\delta = 3.00$ (s, 6H), 6.69 (d, $^3J(H,H) = 9.0$ Hz, 2H), 7.25–7.29 (m, 4H), 8.35 (d, $^3J(H,H) = 8.1$ Hz, 2H), 8.36 (s, 2H), 8.49 (d, $^3J(H,H) = 6.6$ Hz, 2H), 9.09 (d, $^3J(H,H) = 8.1$ Hz, 2H), 9.90 ppm (d, $^3J(H,H) = 5.1$ Hz, 2H); MS (ESI POS): *m/z* (%): 673.1231 $[M]^+$, 451.0076 $[Re(CO)_3(phen)]^+$; elemental analysis calcd (%) for $C_{30}H_{22}N_4O_3RePF_6 \cdot (H_2O)_{0.5}(THF)_{0.5}$: C 44.55, H 3.15, N 6.50; found: C 44.32, H 3.12, N 6.32.

Physical measurements: Aldrich spectroscopic grade or H.P. grade solvents were used for all spectroscopic measurements. Spectral data were analysed by using GRAMS/32 AI (Galactic Industries) software. Mass spectrometry measurements were acquired from a Micromass LCT instrument for electrospray measurements or using a Shimadzu QP8000 alpha with ESI probe. Microanalyses were carried out at the Campbell Microanalysis Laboratory at the University of Otago.

IR spectra were recorded on a Perkin–Elmer Spectrum BX FT-IR System with Spectrum v. 2.00 software. Solid-state samples (KBr disks) were measured over 32 scans at 4 cm^{-1} resolution. FT-Raman spectra were obtained from powder samples of both ligands and complexes on a Bruker IFS-55 interferometer with a FRA/106 attachment. The excitation source was a Nd:YAG laser of wavelength 1064 nm, and a Ge diode (D424) operating at room temperature was used to collect the scattered Raman photons. Spectra were recorded with 64–258 scans, at 4 cm^{-1} resolution and 120 mW laser power at the sample, except for the case of **3** for which the power was reduced to 90 mW to prevent burning. OPUS (version 4.0) software was utilised for the processing of spectra.

Absorption spectra were measured at room temperature on a Varian Cary 500 Scan UV/Vis/NIR spectrophotometer with Cary WinUV scan application software. A scan rate of 600 nm min^{-1} was employed between 200 and 800 nm. Samples were between 10^{-5} and 10^{-6} M in dichloromethane. Solutions were contained in a 1 cm quartz cell.

Resonance Raman spectra were recorded for all complexes by using a set-up described previously.[26] Excitation wavelengths of 351, 413, 444 and 458 nm were employed and solutions were typically 5–7 mM in dichloromethane.

A Perkin–Elmer Luminescence Spectrometer LS50B with FL Winlab v. 4.00.02 software was used to collect steady state fluorescence spectra between 200 and 800 nm. Solutions were ca. 10^{-5}–10^{-6} M in dichloromethane. A range of excitation wavelengths were trialed for each compound, until the strongest emission was obtained. Quantum yields, ϕ, were calculated following the method of Wang et al.,[35] but with 10^{-7} M quinine sulfate in 0.1 M H_2SO_4 as the standard ($\phi = 0.546$).[46]

Transient lifetime (τ) measurements were made at room temperature using a Nd:YAG (Continuum Surelite I-10) pulsed laser (5–7 ns pulse width, operating at 10 Hz). Transient emission signals at 570, 610 and 650 nm were measured with a Hamamatsu fast response (<5 ns) H5783–04 photomultiplier, powered by Hamamatsu 15 V DC power supply and driven at 0.445 V. Spectral discrimination was achieved with a manual mini-chrom (Edmunds Optics) with a 300 μm slit. A notch filter ($\lambda =$

355 nm, Kaiser Optics) was used to remove scattered light. Kinetic traces were recorded using a digital oscilloscope (Tektronix model TDS 3032). Solutions were ca. 10^{-5} M in dichloromethane and were purged with argon for approximately 10 min prior to measurement. The emission lifetime was determined by fitting a single-exponential function to each decay curve. Values were recorded as the mean of the three detection wavelengths, correlated to $[Ru(bipy)]^{2+}$ ($\tau = 0.58$ μs at 25 °C; bipy = bipyridine).[34]

The electrochemical cell for cyclic voltammetry was made up of a 1 mm-diameter platinum rod working electrode embedded in a KeL-F cylinder with a platinum auxiliary electrode and an Ag/AgCl reference electrode. The potential of the cell was controlled by an EG&G PAR 273 A potentiostat with model 270 software. Solutions were typically about 10^{-3} M in dichloromethane with 0.1 tetrabutylammonium perchlorate (TBAP) as the supporting electrolyte, and were purged with nitrogen for approximately 5 min prior to measurement. The scanning speed was 1 V s^{-1}, and the cyclic voltammograms were calibrated against the decamethylferrocenium/decamethylferrocene (DMFc) couple ($E_{ox} = 0.048$ V in CH_2Cl_2 at 100 mV s^{-1}).[47] Results were shifted so that they were relative to the saturated calomel electrode (SCE) by adding 0.045 V.[48]

Computational methods: DFT calculations were performed by using the Gaussian 03 package[49] on the neutral and oxidised ligands and complexes, and on the complexes in their triplet excited state. Previous studies of similar compounds have found the Becke-style 3-parameter DFT method, using the Lee–Parr–Yang correlation functional (B3LYP) with the 6–31G(d) basis set, to be effective in modelling the ligands.[50] The LANL2DZ core potential and associated basis set was used previously to describe the rhenium atom of analogous complexes.[51] This level of theory provides an appropriate balance between accuracy and computational cost for the reasonably large molecules involved. Optimised geometries were used to calculate frequencies of vibrations and their IR and Raman intensities. Importantly, no negative frequencies were obtained in the frequency calculations; this is consistent with an energy minimum for the optimised structure. Frequencies were scaled by a factor of 0.970.[15,52] The MADs for each of the complexes and their free ligands lie between 7–12 cm^{-1}. The values for **4** and each of the doubly and triply bonded species approach the FT-IR and FT-Raman spectral resolution (4 cm^{-1}), suggesting the computational method is accurate in modelling these molecules. The carbonyl modes are quite different in nature to polypyridyl vibrations, thus a separate scale factor would be required to accurately predict their frequencies.[16,53]

Acknowledgements

The support of the Foundation of Research Science and Technology, the Royal Society of New Zealand (Marsden Fund) and the MacDiarmid Institute for Advanced Materials and Nanotechnology is gratefully acknowledged.

[1] C. W. Tang, S. A. VanSlyke, *Appl. Phys. Lett.* **1987**, *51*, 913–915.
[2] H. Yersin, *Top. Curr. Chem.* **2004**, *241*, 1–26.
[3] J.-H. Lee, M.-H. Wu, C.-C. Chao, H.-L. Chen, M.-K. Leung, *Chem. Phys. Lett.* **2005**, *416*, 234–237.
[4] E. Holder, B. M. W. Langeveld, U. S. Schubert, *Adv. Mater.* **2005**, *17*, 1109–1121.
[5] A. Kraft, A. C. Grimsdale, A. B. Holmes, *Angew. Chem.* **1998**, *110*, 416–443; *Angew. Chem. Int. Ed.* **1998**, *37*, 402–428.
[6] N. J. Lundin, A. G. Blackman, K. C. Gordon, D. L. Officer, *Angew. Chem.* **2006**, *118*, 2644–2646; *Angew. Chem. Int. Ed.* **2006**, *45*, 2582–2584.
[7] X. Gong, P. K. Ng, W. K. Chan, *Adv. Mater.* **1998**, *10*, 1337–1340.
[8] W.-Y. Wong, Z. He, S.-K. So, K.-L. Tong, Z. Lin, *Organometallics* **2005**, *24*, 4079–4082.
[9] C. B. Liu, J. Li, B. Li, Z. R. Hong, F. F. Zhao, S. Y. Liu, W. L. Li, *Chem. Phys. Lett.* **2007**, *435*, 54–58.
[10] J. N. Demas, B. A. DeGraff, *Coord. Chem. Rev.* **2001**, *211*, 317–351.
[11] F. Li, M. Zhang, G. Cheng, J. Feng, Y. Zhao, Y. Ma, S. Liu, J. Shen, *Appl. Phys. Lett.* **2004**, *84*, 148–150.
[12] J. R. Schoonover, G. F. Strouse, *Chem. Rev.* **1998**, *98*, 1335–1355.
[13] M. Redecker, D. D. C. Bradley, M. Inbasekaran, W. W. Wu, E. P. Woo, *Adv. Mater.* **1999**, *11*, 241–246.
[14] M. Nomura, K. Fukukawa, Y. Shibasaki, M. Ueda, *Synth. Met.* **2002**, *132*, 9–13.
[15] J. C. Earles, K. C. Gordon, D. L. Officer, P. Wagner, *J. Phys. Chem. A* **2007**, *111*, 7171–7180.
[16] S. L. Howell, K. C. Gordon, *J. Phys. Chem. A* **2006**, *110*, 4880–4887.
[17] T. M. Clarke, K. C. Gordon, D. L. Officer, S. B. Hall, G. E. Collis, A. K. Burrell, *J. Phys. Chem. A* **2003**, *107*, 11505–11516.
[18] L. Sacksteder, A. P. Zipp, E. A. Brown, J. Streich, J. N. Demas, B. A. DeGraff, *Inorg. Chem.* **1990**, *29*, 4335–4340.
[19] M. K. Itokazu, A. S. Polo, N. Y. M. Iha, *J. Photochem. Photobiol. A* **2003**, *160*, 27–32.
[20] A. S. Polo, M. K. Itokazu, K. M. Frin, A. O. d. T. Patrocinio, N. Y. Murakami Iha, *Coord. Chem. Rev.* **2006**, *250*, 1669–1680.
[21] B. Machura, R. Penczek, R. Kruszynski, *Polyhedron* **2007**, *26*, 2470–2476.
[22] M. R. Waterland, S. L. Howell, K. C. Gordon, A. K. Burrell, *J. Phys. Chem. A* **2005**, *109*, 8826–8833.
[23] T. M. Clarke, K. C. Gordon, D. L. Officer, D. K. Grant, *J. Chem. Phys.* **2006**, *124*, 164501 (11 pages).
[24] P. J. Walsh, K. C. Gordon, P. Wagner, D. L. Officer, *ChemPhysChem* **2006**, *7*, 2358–2365.
[25] A. Flood, R. B. Girling, K. C. Gordon, R. E. Hester, J. N. Moore, M. I. J. Polson, *J. Raman Spectrosc.* **2002**, *33*, 434–442.
[26] S. L. Howell, K. C. Gordon, *J. Phys. Chem. A* **2004**, *108*, 2536–2544.
[27] J. R. Lakowicz, *Principles of fluorescence spectroscopy*, Kluwer Academic/Plenum, New York, **1999**.
[28] Excitation at 345 nm produced the most significant emission in **3**, which has an extinction coefficient of 14×10^3 L mol^{-1} cm^{-1} at this wavelength. Therefore in the 2.5×10^{-6} mol L^{-1} solution from which the fluorescence was measured, an absorbance of only 0.035 units is expected across the 1 cm cell. By using $A = -\log(I/I_o)$, this corresponds to an I/I_o of 0.92.
[29] X. Zhou, J.-K. Feng, A.-M. Ren, *Chem. Phys. Lett.* **2005**, *403*, 7–15.
[30] Y. H. Park, H. H. Rho, N. G. Park, Y. S. Kim, *Curr. Appl. Phys.* **2006**, *6*, 691–694.
[31] W. M. Xue, N. Goswami, D. M. Eichhorn, P. L. Orizondo, D. P. Rillema, *Inorg. Chem.* **2000**, *39*, 4460–4467.
[32] E. M. Kober, J. L. Marshall, W. J. Dressick, B. P. Sullivan, J. V. Caspar, T. J. Meyer, *Inorg. Chem.* **1985**, *24*, 2755–2763.
[33] J. V. Caspar, T. J. Meyer, *J. Phys. Chem.* **1983**, *87*, 952–957.
[34] J. Van Houten, R. J. Watts, *J. Am. Chem. Soc.* **1975**, *97*, 3843–3844.
[35] K. Wang, L. Huang, L. Gao, L. Jin, C. Huang, *Inorg. Chem.* **2002**, *41*, 3353–3358.
[36] B. C. Lin, C. P. Cheng, Z. P. M. Lao, *J. Phys. Chem. A* **2003**, *107*, 5241–5251.
[37] E. T. Seo, R. F. Nelson, J. M. Fritsch, L. S. Marcoux, D. W. Leedy, R. N. Adams, *J. Am. Chem. Soc.* **1966**, *88*, 3498–3503.
[38] W. B. Connick, A. J. Di Bilio, M. G. Hill, J. R. Winkler, H. B. Gray, *Inorg. Chim. Acta* **1995**, *240*, 169–173.
[39] Y. F. Li, Y. Cao, J. Gao, D. L. Wang, G. Yu, A. J. Heeger, *Synth. Met.* **1999**, *99*, 243–248.
[40] H. Gilman, G. Karmas, *J. Am. Chem. Soc.* **1945**, *67*, 342.
[41] K. Kondo, N. Ohnishi, K. Takemoto, H. Yoshida, K. Yoshida, *J. Org. Chem.* **1992**, *57*, 1622–1625.
[42] X. Zhang, Y. Sun, Y. Wu, Y. Feng, X. Tao, M. Jiang, *Mater. Lett.* **2005**, *59*, 3458–3488.
[43] U. Hess, D. Huhn, *J. Prakt. Chem.* **1983**, *325*, 301–308.
[44] M. J. G. Lesley, A. Woodward, N. J. Taylor, T. B. Marder, I. Cazenobe, I. Ledoux, J. Zyss, A. Thornton, D. W. Bruce, *Chem. Mater.* **1998**, *10*, 1355–1365.
[45] N. J. Lundin, P. J. Walsh, S. L. Howell, J. J. McGarvey, A. G. Blackman, K. C. Gordon, *Inorg. Chem.* **2005**, *44*, 3551–3560.
[46] C. C. Clark, G. J. Meyer, Q. Wei, E. Galoppini, *J. Phys. Chem. B* **2006**, *110*, 11044–11046.

[47] I. Noviandri, K. N. Brown, D. S. Fleming, P. T. Gulyas, P. A. Lay, A. F. Masters, L. Phillips, *J. Phys. Chem. B* **1999**, *103*, 6713–6722.
[48] D. Bard, J. Yarwood, B. Tylee, *J. Raman Spectrosc.* **1997**, *28*, 803–809.
[49] Gaussian 03, Revision C.02, M. J. Frisch, G. W. Trucks, H. B. Schlegel, G. E. Scuseria, M. A. Robb, J. R. Cheeseman, J. A. Montgomery, Jr., T. Vreven, K. N. Kudin, J. C. Burant, J. M. Millam, S. S. Iyengar, J. Tomasi, V. Barone, B. Mennucci, M. Cossi, G. Scalmani, N. Rega, G. A. Petersson, H. Nakatsuji, M. Hada, M. Ehara, K. Toyota, R. Fukuda, J. Hasegawa, M. Ishida, T. Nakajima, Y. Honda, O. Kitao, H. Nakai, M. Klene, X. Li, J. E. Knox, H. P. Hratchian, J. B. Cross, C. Adamo, J. Jaramillo, R. Gomperts, R. E. Stratmann, O. Yazyev, A. J. Austin, R. Cammi, C. Pomelli, J. W. Ochterski, P. Y. Ayala, K. Morokuma, G. A. Voth, P. Salvador, J. J. Dannenberg, V. G. Zakrzewski, S. Dapprich, A. D. Daniels, M. C. Strain, O. Farkas, D. K. Malick, A. D. Rabuck, K. Raghavachari, J. B. Foresman, J. V. Ortiz, Q. Cui, A. G. Baboul, S. Clifford, J. Cioslowski, B. B. Stefanov, G. Liu, A. Liashenko, P. Piskorz, I. Komaromi, R. L. Martin, D. J. Fox, T. Keith, M. A. Al-Laham, C. Y. Peng, A. Nanayakkara, M. Challacombe, P. M. W. Gill, B. Johnson, W. Chen, M. W. Wong, C. Gonzalez, J. A. Pople, Gaussian, Inc., Pittsburgh, PA, **2004**.
[50] B. J. Matthewson, A. Flood, M. I. J. Polson, C. Armstrong, D. L. Phillips, K. C. Gordon, *Bull. Chem. Soc. Jpn.* **2002**, *75*, 933–942.
[51] D. M. Dattelbaum, R. L. Martin, J. R. Schoonover, T. J. Meyer, *J. Phys. Chem. A* **2004**, *108*, 3518–3526.
[52] A. P. Scott, L. Radom, *J. Phys. Chem.* **1996**, *100*, 16502–16513.
[53] P. S. Braterman, *Metal Carbonyl Spectra*, Academic Press, London, **1975**.

Received: November 14, 2008
Published online: March 5, 2009

